Archives of Virology (2018) 163:2687–2699
https://doi.org/10.1007/s00705-018-3911-x

ORIGINAL ARTICLE

Zika-virus-infected human full-term placental explants display pro-inflammatory responses and undergo apoptosis

Milene Rocha Ribeiro[1,6] · Jusciele Brogin Moreli[2] · Rafael Elias Marques[3] · Michelle Premazzi Papa[4] · Lana Monteiro Meuren[4] · Paula Rahal[1] · Luciana Barros de Arruda[4] · Antonio Helio Oliani[6] · Denise Cristina Mós Vaz Oliani[6] · Sonia Maria Oliani[1] · Aarthi Narayanan[5] · Maurício Lacerda Nogueira[6]

Received: 3 October 2017 / Accepted: 31 May 2018 / Published online: 6 June 2018
© Springer-Verlag GmbH Austria, part of Springer Nature 2018

Abstract

Zika virus (ZIKV) is a flavivirus that has been highly correlated with the development of neurological disorders and other malformations in newborns and stillborn fetuses after congenital infection. This association is supported by the presence of ZIKV in the fetal brain and amniotic fluid, and findings suggest that infection of the placental barrier is a critical step for fetal ZIKV infection *in utero*. Therefore, relevant models to investigate the interaction between ZIKV and placental tissues are essential for understanding the pathogenesis of Zika syndrome. In this report, we demonstrate that explant tissue from full-term human placentas sustains a productive ZIKV infection, though the results depend on the strain. Viral infection was found to be associated with pro-inflammatory cytokine expression and apoptosis of the infected tissue, and these findings confirm that placental explants are targets of ZIKV replication. We propose that human placental explants are useful as a model for studying ZIKV infection *ex vivo*.

Introduction

Zika virus (ZIKV), a member of the family *Flaviviridae*, is an enveloped, single-strand RNA virus that was the causative agent of major outbreaks in the Americas in 2015 [57, 69]. Its genome has a typical flavivirus architecture and is approximately 11 kb in length. The virus was first isolated from a Rhesus Macaque in 1947 in the Zika forest in Uganda; however, ZIKV infection had been poorly investigated until recently, when numerous infections were reported in more than 60 countries and territories around the world. Major outbreaks have been recorded on the Yap Islands (2007), in French Polynesia (2013), and in Brazil (2015). The virus is primarily transmitted by *Aedes aegypti* mosquitoes, and humans are considered to be amplification hosts, though nonhuman primates may be involved in maintenance of the virus in Africa [68]. In addition, the virus is unique in relation to other flaviviruses such as dengue virus (DENV) in that it may be transmitted by alternative routes, including through sexual and maternal-fetal routes [20, 21, 64, 71].

Most of the cases associated with ZIKV infection are either asymptomatic or present only mild symptoms such as fever, rash, joint pain, and conjunctivitis. Myalgia and headaches have also been reported. In recent outbreaks,

Handling Editor: Tim Skern.

Electronic supplementary material The online version of this article (https://doi.org/10.1007/s00705-018-3911-x) contains supplementary material, which is available to authorized users.

✉ Maurício Lacerda Nogueira
mnogueira@famerp.br

[1] Department of Biology, School of Biosciences, Humanities and the Exact Sciences, São Paulo State University (UNESP), São José do Rio Preto, São Paulo, Brazil

[2] Federal University of São Paulo (UNIFESP), São Paulo, São Paulo, Brazil

[3] Brazilian Biosciences National Laboratory (LNBio), National Center for Research in Energy and Materials (CNPEM), Campinas, São Paulo, Brazil

[4] Paulo de Góes Department of Microbiology, Federal University of Rio de Janeiro (UFRJ), Rio de Janeiro, Brazil

[5] George Mason University, Fairfax, Virginia, USA

[6] Virology Research Laboratory, Department of Dermatological, Infectious, and Parasitic Diseases, São José do Rio Preto School of Medicine (FAMERP), São José do Rio Preto, São Paulo, Brazil

however, ZIKV infection was highly correlated with neurological manifestations, particularly in developing fetuses after congenital infection [4, 9, 44]. In fact, infection of pregnant women has been associated with miscarriage, fetal abnormalities, microcephaly, and other neurological diseases in newborns [41, 53]. The virus has been isolated from multiple bodily fluids from infected individuals, including serum, urine, saliva, and semen [48]. Importantly, the virus has also been detected in amniotic fluid and in the brains of microcephalic newborns and fetuses in cases of stillbirth [7, 46], demonstrating that ZIKV crosses the placenta through an unknown mechanism of action.

Recent studies using experimental mouse models have also indicated that the virus might cross the placental barrier, leading to congenital ZIKV transmission. Systemic infection of pregnant mice resulted in abnormal brain development and microcephaly in the offspring, outcomes that were attributed to viral neurotropism [14, 45, 72]. Infection of trophoblasts and endothelial cells in the placentas of ZIKV-infected mice and nonhuman primates have also been reported [1, 45, 54].

However, most animal models used to study ZIKV infection are deficient in the expression of type I or type I and type II interferon receptors (A129 and AG129, respectively) [2, 45, 59]. Mice that lack components of innate immune responses, including *Mavs*$^{-/-}$, *Irf3*$^{-/-}$, *Irf3*$^{-/-}$*Irf5*$^{-/-}$*Irf7*$^{-/-}$, have also shown susceptibility to ZIKV infection [37]. Although these models are useful for evaluating the efficacy of vaccine candidates and therapies, they may not represent the true effects associated with trans-placental transmission of the virus in immunocompetent individuals, or the conditions in the placenta that favor viral multiplication, including possible local inflammation.

A critical unmet need is a model that can be used to quickly, quantitatively, and effectively screen for functionally relevant countermeasures that may protect the fetus from intrauterine transmission of ZIKV. In this report, we demonstrate that placental explants obtained from full-term placental tissue both support and are affected by ZIKV infection. This tissue may be useful as a model for such experimentation, as well as for the development of treatments against ZIKV infections.

Materials and methods

Cell lines and viruses

Vero cells were cultivated in MEM supplemented with 10% fetal bovine serum, 100 units of penicillin per mL, and 100 µg of streptomycin per mL at 37 °C in a humidified atmosphere containing 5% CO_2. ZIKV-BR (GenBank accession number KU497555; kindly provided by Pedro Vasconcelos, Evandro Chagas Institute, FIOCRUZ, Pará, Brazil) was isolated from a mild case of ZIKV in the state of Paraíba, Brazil, and it was distributed within our local research network project after four passages in C6/36 cells [18]. The DENV-2 strain used was New Guinea C, or NGC (GenBank accession number AF038403). The viruses were propagated and titrated using Vero cells. The viral stock was aliquoted in 100-µL portions and stored at − 80 °C. Titers were determined and titrated using a standard $TCID_{50}$ assay.

Infections in human placental explant cultures

Normal human placenta tissues were obtained from full-term elective cesarean deliveries in cases of non-labor after 38 to 40 weeks of gestation (n = 10) at the Children's and Maternity Hospital of São José do Rio Preto, São Paulo, Brazil, after approval from the local research ethics committee. Placentas were processed within 15 min of delivery. Chorionic villi were dissected into 5-mm sections, and tissues were washed extensively with PBS (1x). Explants were cultured in standard tissue culture plates in DMEM (Cultilab) combined with Ham's F-12 Nutrient Mixture (HAMF-12; Thermo Fisher) and supplemented with 10% FBS (GIBCO), 1% penicillin-streptomycin, and 100 mg of gentamicin per mL. Cultures were maintained at 37 °C in a humidified atmosphere containing 5% CO_2. Twenty-four hours after plating, samples were infected with 1×10^4 TCD_{50} of ZIKV-BR or DENV2. The culture was incubated for 4 hours to allow for virus adsorption. The explants were then washed three times with PBS (1X) for complete removal of the inoculum. The explants were then maintained in DMEM/HAMF-12 with 2% FBS. Culture supernatants from infected and uninfected explants were collected at 0, 3, 6, 12, 24, 72, and 120 hours postinfection (hpi) without the addition of fresh media or washing. Explants were then collected to determine total RNA and were fixed in 4% paraformaldehyde for histology and immunohistochemistry analysis. The culture medium was collected to perform plaque assays and to quantify β-hCG through the use of electrochemiluminescence (Roche Hitachi, Cobas® e411). Some sample tissues that had been cultured for 24 hours were also treated with neutralizing anti-TNF RII/TNFRSF1B antibody (100 ng/mL, R&D Systems, Minneapolis, MN, USA) or TLR-3 ligand polyinosinic:polycytidylic acid, or poly (I:C) (50 µg/mL; Sigma-Aldrich) for 24 hours.

Viral quantification

ZIKV RNA was quantified from culture supernatants using a TaqMan-based qRT-PCR assay (GoTaq ® Probe 1-Step RT-qPCR System, REF AG120) as described previously [35]. DENV2 RNA was analyzed using a SuperScript III Platinum SYBR Green One Step RT-qPCR Kit (REF 1136-059) and

the primers described by Chutinimitkul and colleagues [11]. The primer and probe sequences are described in supplementary Table A1.

Plaque assay

Vero cells were plated at a density of 5×10^5 cells per well in a six-well plate and cultured for 24 hours at 37°C under 5% CO_2. Serial dilutions of supernatant from explant cultures (24 and 72 hpi) were added to each well for 1 hour of incubation. After the medium was removed, infected monolayers were covered with 1.5% carboxymethylcellulose (CMC)/MEM with 2% FSB at a 1:1 ratio. Plaque foci were detected on day 5 after fixation with 10% formalin solution and staining with 2% crystal violet.

Histological analysis

Infected placental tissue sections and their uninfected controls were fixed in 4% buffered formalin for 24 hours, dehydrated in graded ethanol, and embedded in paraffin for histopathological analysis. The samples were stained with hematoxylin and eosin (H&E) and analyzed using a high-power objective (20×) on an Axioskop 2-Mot Plus Zeiss microscope (Carl Zeiss, Jena, Germany). To quantify nuclear fragmentation, 10 random photos were taken of experiments performed in triplicate, and the amount of karyorrhexis was determined for each photo. The mean plus or minus standard deviation per field is shown.

Immunohistochemistry

ZIKV infection and caspase-3 activation were analyzed in the placental explants using immunohistochemistry. Sections of infected placental tissue and the uninfected controls were collected at 72 and 120 hpi. Some samples were also treated with neutralizing anti-TNFRII/TNFRSF1B antibody (R&D Systems, Minneapolis, MN) and harvested at 72 hpi. Serial 3-µm-thick tissue sections were deparaffinized and rehydrated prior to antigen retrieval in citrate buffer at a pH of 6.0. Endogenous peroxide activity was blocked with 3% hydrogen peroxide for 30 minutes, followed by blocking with 10% bovine serum albumin (BSA; Sigma-Aldrich, Missouri, USA) in Tris-buffered saline (TBS) for 2 hours. The slides were incubated with primary mouse antibody against flavivirus E protein (4G2) at a dilution of 1:100, anti-caspase-3 (Abcam, cat. number ab2302) at 1:200, anti-cytokeratin 7 (Dako) at 1:250, or anti-vimentin (Dako) at 1:150 in 10% TBS-BSA for 1 hour at 37 °C, all of which were applied in independent trials. After the washing step, sections were incubated with a secondary antibody (HRP-conjugated anti-mouse or anti-rabbit antibody; Abcan). Positive staining was detected using 3,3′-diaminobenzidine (DAB substrate; Invitrogen, USA). Finally, sections were counterstained with H&E (hematoxylin from InlabConfiança and eosin from AnalytiCals). A negative reaction control was run in the absence of primary antibodies. Analysis was performed using an Axioskop 2-Mot Plus microscope (Carl Zeiss, Jena, Germany) and AxioVision software for densitometric and quantitative analysis. The experiments were each performed in triplicate using samples from three individual donors, and ten fields were quantified in each section. Densitometric analysis was used to determine caspase-3 and 4G2 intensity in sections of placental tissue (40×) on an arbitrary scale from 0 to 255, and the data were expressed as the mean plus or minus standard deviation [6].

Cytokine gene relative expression analysis

RNA from virus-infected explants and uninfected controls was extracted using TRIzol according to the manufacturer's instructions (Life Technologies). Likewise, RNA was extracted within 24 hours from uninfected samples treated with 50 µg of poly (I:C) per mL, as well as from the untreated controls. Cytokine gene relative expression analyses were performed using a SuperScript III Platinum SYBR Green One Step qRT-PCR Kit (Invitrogen; REF 1136-059). The primer sequences for the IL-6, IL-10, IL-1β, TNF-α, IFN-β, IFN-γ, IFN-λ1, and IFN-λ4 cytokines are listed in supplementary Table A2. A comparative ΔΔCt method was used to quantify gene expression levels based on GAPDH Ct values for normalization.

TUNEL assay

Detection of nuclear DNA fragmentation as a morphological marker of the apoptosis process in histological sections was performed using a TUNEL assay. The assay was performed using an In Situ Cell Death Detection Kit (TMR red). After 3 days of infection, 3-mm infected tissue sections and uninfected controls were deparaffinized, hydrated, and rinsed with 0.1 M phosphate buffer (pH 7.4), followed by blocking with 3% BSA and 20% FBS. TUNEL reaction mixture (TdT enzyme fluorescein-labeled nucleotide mix) was added, and the sections were incubated for 60 minutes at 37 °C. For the positive reaction control, the sections were treated with 3U of DNase I per mL for 10 minutes at room temperature. Quantitative analysis was performed using Image-Pro® Plus image analysis software, and fluorescent images of TUNEL-positive cells were captured using an Olympus BX53 microscope system at 40× in red channel detection in the range of 570 to 620 nm. Tests were performed in duplicate, and images of three random fields were acquired from each slide to calculate the mean plus or minus standard deviation.

Data analysis

Data were analyzed using GraphPad Prism software (version 6; GraphPad, CA). Results are expressed as the mean plus or minus standard deviation. Data were analyzed using one-way ANOVA followed by the non-parametric Kruskal-Wallis test (unpaired data) or the Bonferroni correction. Data from a minimum of three independent experiments are presented. Significance was established as $p < 0.05$.

Results and discussion

Placental explants support ZIKV infection

Our goal was to determine whether explants of human placental tissue are a useful model for studying ZIKV infection *ex vivo*. To that end, normal full-term placental tissues were obtained following cesarean section. Chorionic villi were dissected, and the explants (5 mm) were infected with ZIKV-BR or dengue virus 2 (DENV2) for comparison. Immunostaining of the tissues at 72 hpi with the anti-flavivirus antibody 4G2 demonstrated that the tissues were infected by both viruses (Fig. 1a-d). To confirm that placental explants would support a progressive ZIKV infection, culture supernatants from these infected explants were obtained at 0, 3, 6, 12, 24, 72, and 120 hpi, and virus RNA levels were analyzed using RT-qPCR (Fig. 1e). We observed a progressive increase in the ZIKV RNA load as early as 12 hpi, with a peak at 72 hpi. DENV 2 RNA was also detected in placental supernatants until 24 hpi, but RNA levels did not increase at the subsequent time points. Culture supernatants from infected tissues collected at 0 hpi exhibited a viral load of $< 10^1$, and this value was subtracted from those obtained at subsequent time points. Uninfected tissues exhibited no viral load when measured using RT-qPCR.

The release of infectious virus particles at different time points after infection was also evaluated using plaque assay. Accordingly, we observed increased levels of ZIKV plaque-forming units (PFU) in the supernatants of explanted tissues, whereas DENV2 PFU levels decreased at later time points (Fig. 1f).

H&E staining and histological analysis demonstrated that placental tissues infected with ZIKV-BR showed signs of cellular injury, in contrast to uninfected tissues (Fig. 2a-c; additional images can be found in Figure A3 of the Supplementary Information). The presence of trophoblasts in these sections was confirmed by the high expression of the cytokeratin-7 epithelial cell marker (Fig. 2d-f), as well as by the absence of vimentin expression (mesenchymal cell marker) (Fig. 2g-i). In addition, the quantification of nuclear fragmentation revealed a larger amount of karyorrhexis in ZIKV-BR infection than in uninfected and DENV-infected tissues, a finding that suggests that viral replication may indeed be associated with tissue damage (Fig. 2j).

Other studies have demonstrated that placental explant cultures secrete hCG during the process of explant re-epithelization [31, 34, 47, 67]. We evaluated whether ZIKV infection would affect the secretion of b-hCG, a marker of syncytiotrophoblast (SCT) renewal and viability (Fig. 2d-i, k) [32]. ZIKV-infected tissues exhibited lower b-hCG secretion in the culture than the uninfected control (Fig. 2k), a result that suggests lower SCT recovery upon ZIKV infection. Meanwhile, DENV-infected tissues exhibited lower b-hCG secretion after 48 h, thus reducing SCT viability. However, SCTs were found to increase secretion of b-hCG 72 h after infection, suggesting improved SCT recovery. These findings are in accordance with previous studies on experimental mouse models, the results of which have demonstrated the infection of fetal and maternal placental tissues [45]. These and other experimental models have also shown that ZIKV infects various primary human placental cell types and chorionic villus explants, and the data are suggestive of infection occurring via placental and paraplacental virus transmission routes [56, 63]. Previous studies have reported that both cytotrophoblasts (CTBs) and SCTs from chorionic villi exhibit E protein expression upon ZIKV infection; however, only CTBs expressed the nonstructural protein NS3 [63]. In addition, it has been proposed that trophoblasts are resistant to ZIKV replication, based on a study showing that different trophoblast-derived cell lines were permissive to ZIKV, while human primary trophoblasts exhibited low viral RNA levels when compared to other cell types [3]. On the other hand, both macrophages and CTBs obtained from the same tissues were found to be susceptible to ZIKV [56].

An experimental model involving pregnant rhesus monkeys revealed prolonged viremia compared to non-pregnant animals, and the use of this system has provided important data on ZIKV infection in the first and third trimesters. These data show that placentas from late-stage pregnancies are still vulnerable to ZIKV. Therefore, models of infection in full-term explants can be used to recapitulate the second half of pregnancy. Furthermore, full-term explants have the advantage of being easy to obtain after delivery [13, 54].

Our data clearly demonstrate that full-term human placenta explants are permissive to ZIKV and DENV2 infections, which are associated with cell injury. Discrepancies between different studies may be attributed to the time at which the explant was obtained and to the specific ZIKV strain used. It is important to note that immunohistochemical staining and progressive RNA release from cultures indicate that this model can be used to study the dynamics of infection and of host-virus interaction.

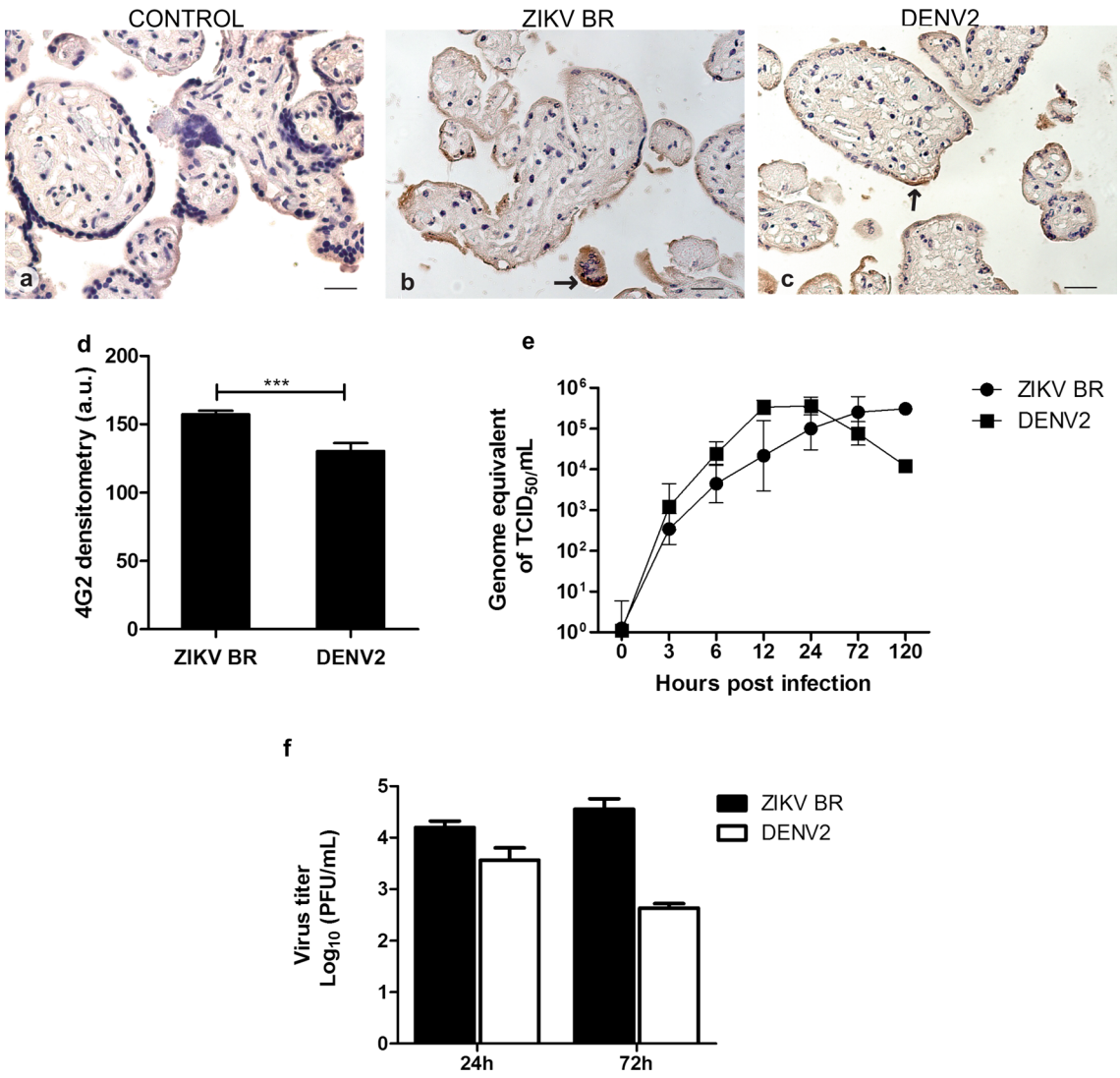

Fig. 1 ZIKV productively infects human placental tissue explants. Placental explants were left uninfected (control) (**a**) or infected with ZIKV (**b**) or DENV (**c**) at 1×10^4 $TCID_{50}$. After 72 hpi, immunohistochemistry staining was performed using the anti-flavivirus 4G2 antibody. Black insets show the details of immunohistochemistry staining. Quantification of 4G2 staining using densitometry in arbitrary units (a.u.) was performed using an Axioskop 2-Mot Plus Microscope (Carl Zeiss, Jena, Germany). The AxioVision software was used for qualitative analysis. Densitometry analysis of the reaction-negative control and of the uninfected samples consistently produced negative results. The data were analyzed using one-way ANOVA followed by the Kruskal-Wallis test; ***, $p < 0.001$ (**d**). Full-term placental explants were left uninfected (controls) or were infected with ZIKV-BR or DENV2 viruses (1×10^4 $TCID_{50}$), and the supernatants were harvested at the time points indicated. RNA extraction and qRT-PCR were performed using specific ZIKV and DENV primers as described in Materials and methods (**e**). The titers of infectious particles in the supernatants were evaluated by plaque assay in Vero cells (**f**). All of the data were obtained from experiments performed in triplicate and are represented as the mean +/− standard deviation. Scale bar: 10 μm

ZIKV infection induces cytokine expression in placental explants

Placental damage and dysfunction caused by viral infection may be a consequence of the viral cytopathic effect or host-mediated pathology [28]. Such conditions alter placental development, restrict fetal growth [42], and may result in neuroinflammation [66]. To determine whether antiviral or inflammatory responses to infection are related to placental dysfunction, we evaluated the expression of interferons (IFNs) and pro-inflammatory cytokines in ZIKV-infected placenta explants.

ZIKV infections in other experimental models have been associated with increased expression of innate immune sensors and interferon-stimulated genes [27]. Also, studies have found purified primary human trophoblasts and trophoblast-derived cell lines to be resistant to ZIKV infection due to the production of type III IFNs (IFN-λ1 and -λ2)

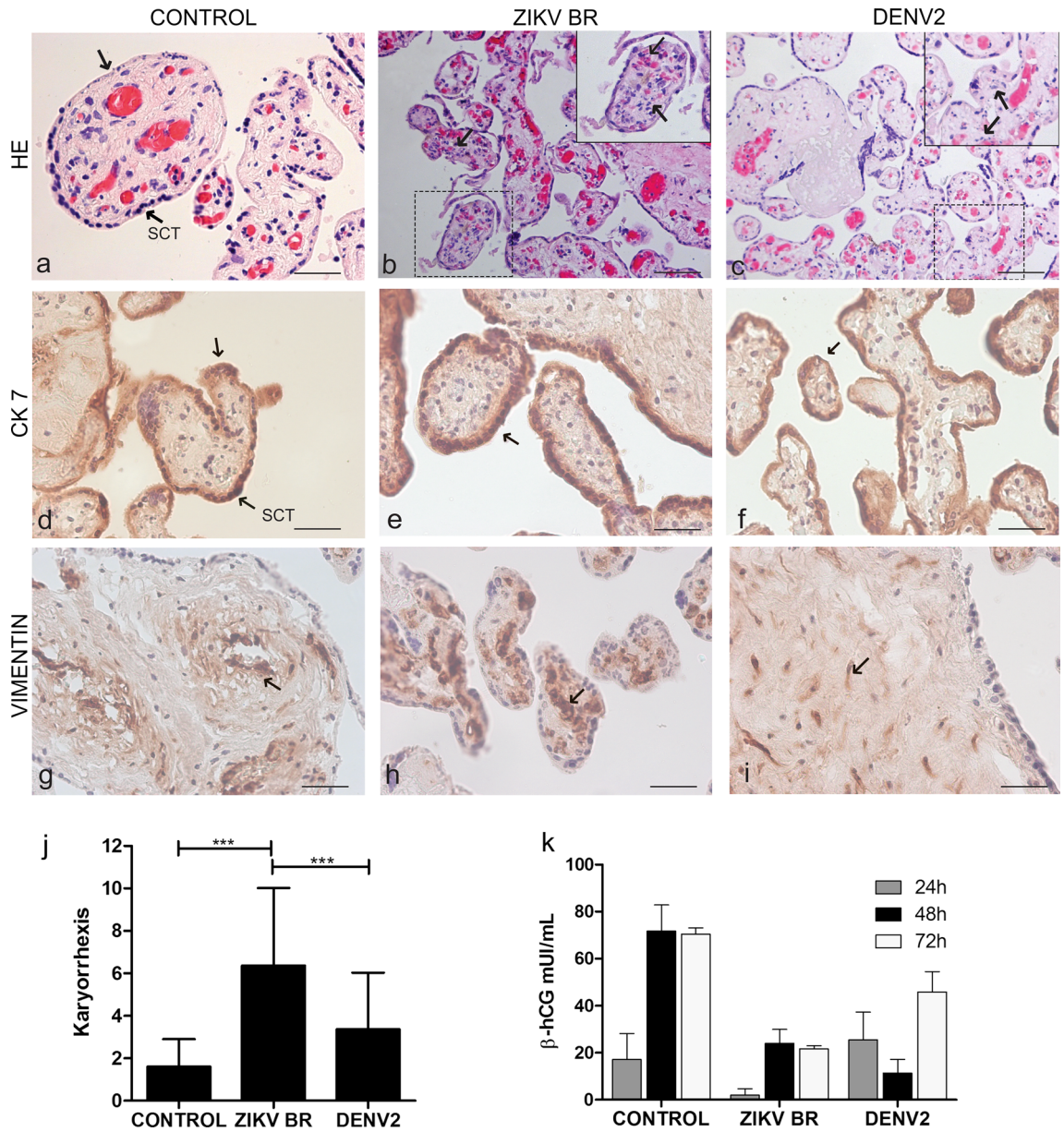

Fig. 2 Histological analysis of infected placental explants. Human placental explants were left uninfected (control) or were infected with ZIKV or DENV. After 72 hpi, immunohistochemistry analysis was performed. The tissues were stained with H&E. Black arrows indicate karyorrhexis, and red arrows point to stromal injury. SCT: syncytiotrophoblasts (**a-c**). Immunohistochemistry analysis of the placental tissues stained with anti-cytokeratin (CK7); black arrows indicate cells stained with anti-cytokeratin (CK7) (**d-f**). Immunohistochemistry analysis of the placental tissues stained with anti-vimentin (mesenchymal cells); black arrows indicate cells stained with anti-vimentin (**g-i**). The graph represents the mean +/− standard deviation of the number of cells per field, with karyorrhexis detected in ten random photos taken from experiments performed in triplicate in the H&E analysis (**j**). The data were analyzed using one-way ANOVA followed by the Bonferroni correction; ***, $p < 0.001$. β-hCG was quantified to determine SCT viability (**k**). Scale bar: 10 µm

[3]. Our experimental model supports ZIKV replication, so we investigated whether and how the relative expression of type I (IFN-β), type II (IFN-γ), and type III (IFN-λ1 and λ4) IFNs would take place in infected placental explants. As a positive control of IFN expression, we cultured explants with poly(I:C) and observed an increase in IFN-β, IFN-λ1, IFN-λ4 and IFN-γ expression at 24 hpi relative to untreated cultures (Fig. 3a). Notably, IFN-λ4 and IFN-γ reached higher levels of expression than IFN-β and IFN-λ1. Placental explants were also infected with ZIKV or DENV or left uninfected, and IFN expression was evaluated at 24 and 72 hpi. ZIKV and DENV infections induced a mild increase in IFN-λ1 and IFN-λ4 expression at 24 hpi; the exception was IFN-λ4 in the case of DENV infection, which did not

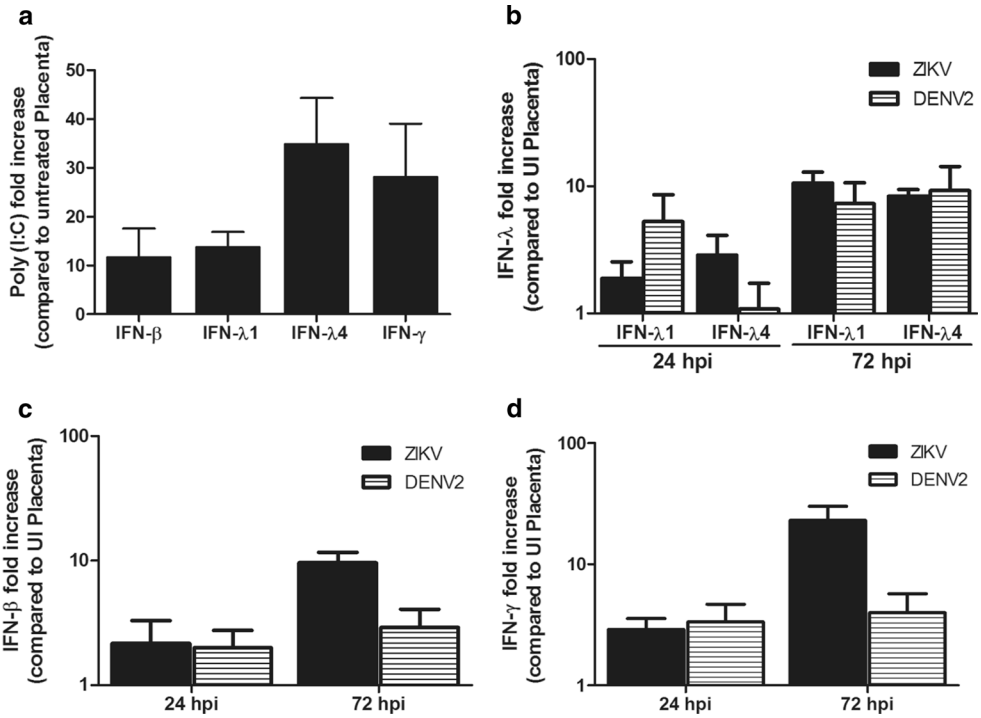

Fig. 3 IFN relative expression in infected placental tissue explants. Explants were cultured with poly(I:C) for 24 hours. RNA was extracted, and the IFN mRNA levels were analyzed by quantitative RT-PCR and normalized using the housekeeping gene GAPDH (**a**). Explants were cultured with ZIKV or DENV for 24 or 72 h. Next, RNA was extracted, and mRNA levels of IFN- λ1 and IFN- λ4 (**b**), IFN- β (**c**), and IFN-γ (**d**) were analyzed by quantitative RT-qPCR and normalized by GAPDH. Results are shown as fold change relative to controls consisting of uninfected tissues and unstimulated poly(I:C). The data shown are representative of at least three independent experiments and are presented as the mean +/− standard deviation

increase (Fig. 3b). At 72 hpi, IFN-λ1 and IFN-λ4 expression in infected explants increased as much as tenfold in the cases of both viral infections. Type III IFNs include IFN-λ1, λ2/λ3, and λ4, all of which seem to induce a similar antiviral response pattern mediated by IFNLR1/IL-10R2 engagement and activation of the JAK-STAT signaling pathway, thus leading to ISG expression [29, 33, 43]. Several studies based on different infectious models have demonstrated that IFN-λ1 and IFN-λ2/λ3 are similarly regulated by IRF-3 and IRF-7 activation. These results strongly suggest that type I and III IFN genes are regulated by a common mechanism. [38].

Despite the differential activation of IFN-λ1 and IFN-λ2, detailed analyses are needed to elucidate the mechanism of this activation. Influenza A virus induces the expression of IFN-λ1 (but not IFN-λ2), although Sendai virus has been found to induce production of high levels of IFN-λ1 and IFN-λ2 [50].

In the infection of both trophoblast cell lines and primary human trophoblasts with ZIKV, the secretion of IFN-λ1 and IFN-λ2 was constitutive. This result demonstrates the important role of interferon-type-III-mediated protection from ZIKV infections at the maternal–fetal interface [3, 12].

IFN-λ4 was discovered more recently, and there is evidence that its expression is regulated by a transduction signaling pathway similar to those regulating other type III IFNs [38, 52]. Our data demonstrated that type III IFNs were produced in the placental explant model and increased over the time points evaluated, and this is consistent with previous data obtained from the use of other placental culture models [3, 12]. The activation of the type III IFN-inducing pathway was further demonstrated by the increased levels of IFN-λ4 mRNA, the expression of which seems not to have been evaluated for ZIKV infection prior to this study. Any discrepancies between our results and those in the literature could be attributed to factors such as the use of different ZIKV strains and the use of a placental explant rather than a single epithelial cell type from the placenta.

ZIKV and DENV2 also induced mild increases in IFNβ expression at 24 hpi, and there was a subsequent significant increase in IFNβ expression at 72 hpi only in the ZIKV-infected explants (Fig. 3c). Interestingly, our results on IFN-γ expression showed a similar pattern, in which only ZIKV infection caused an increase in IFN expression at 72 hpi (Fig. 3d). IFN-γ may induce apoptosis of human primary trophoblasts, mediate proliferation and migration of extravillous cytotrophoblasts (EVCT), and, when in excess, be harmful to pregnancy and to fetal growth [36, 65, 70]. ZIKV NS5 has been found to destabilize STAT2 and suppress the signaling mediated by type I and type III IFN [5, 10, 56]. Therefore, increased levels of IFNs produced to restrict ZIKV infection may be counteracted by the virus while also inducing inflammation and other host responses that could have deleterious effects on pregnancy.

To investigate other aspects of the immune response to ZIKV in placental explants, we assessed the relative expression of IL-1β, IL-6, IL-10, and TNF-α in ZIKV-infected tissues (Fig. 4). Tissues were either stimulated with poly(I:C) or infected with ZIKV or DENV. All groups exhibited increased expression of all of the cytokines evaluated (IL-1β,

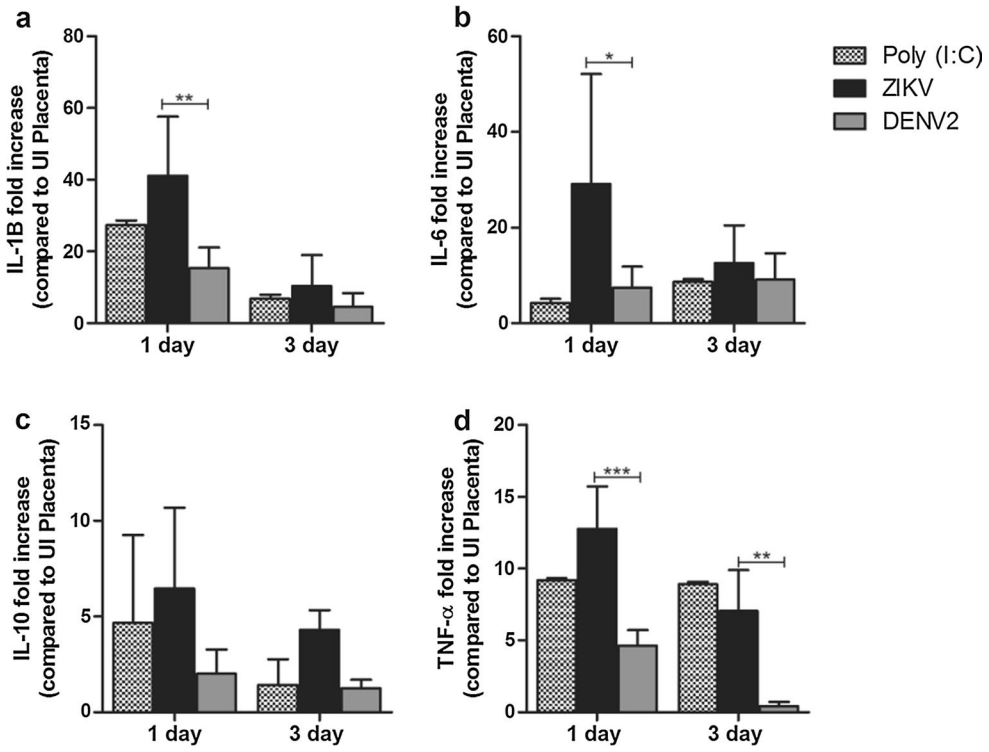

Fig. 4 Cytokine relative expression profiles in placental tissue explants. ZIKV-BR- and DENV2-infected explants were analyzed for cytokine gene expression using RT-qPCR. Uninfected explants (UI) and poly(I:C)-stimulated tissues were analyzed as negative and positive controls, respectively. Unstimulated poly(I:C) and uninfected tissues were used to compare the fold increase. Total RNA was extracted from the explants on days 1 and 3 postinfection. The RNA levels for IL-1β (**a**), IL-6 (**b**), IL-10 (**c**), and TNF-α (**d**) were quantified using gene-specific primers. The analysis was performed using samples obtained in triplicate. Data are represented as the mean +/− standard deviation. One-way ANOVA was performed, followed by Bonferroni correction. *, $p < 0.05$; **, $p < 0.01$; and ***, $p < 0.001$ were considered significant

IL-10, IL-6, and TNF-α) upon infection/stimulation relative to uninfected controls. At 1 day postinfection (dpi), ZIKV-infected explants exhibited significantly higher expression of IL-1β, IL-6, and TNF-α in comparison to DENV2-infected explants (Fig. 4a, b, and d). The expression of pro-inflammatory cytokines such as IL-1β, IL-6, and TNF-α alters the intra-amniotic milieu and is a marker of fetal inflammatory response syndromes. Increased Th1 cytokines have been associated with spontaneous preterm labor and with disruption of fetal tolerance [17, 22, 58]. IL-1β has also been associated with the expression of metalloproteinases and CTB invasion during pregnancy [40, 55]. *In vitro* treatment with IL-1RA impaired trophoblast fusion, viability, and hCG secretion, indicating that IL-1B plays an important role in placental dysfunction and adverse pregnancy outcomes [15, 24]. TNF-α expression during pregnancy is associated with detrimental effects, including gestational hypertension and gestational diabetes mellitus [26, 30, 62]. TNF-α may act directly upon early-term placentas and cause placental pathology, fetal hypoxia, and neurodevelopmental defects in the fetal brain [8]. Also, TNF-α disturbs trophoblast function, leading to decreased cell fusion and reduced expression of hCG [39, 51]. TNFα may also be associated with cell death, as described in other models [23]. IL-10, on the other hand, is typically anti-inflammatory, which often results in tissue protection and is involved in fetal tolerance [19, 60, 61]. ZIKV infection induced the expression of significant levels of pro-inflammatory cytokines, but not of IL-10. This combination could result in pathology and may account for some of the deleterious effects of ZIKV infection during pregnancy.

DENV2 was not able to induce the expression of pro-inflammatory cytokines to the same levels as ZIKV, a difference that may be associated with lower replication efficiency and consequent lower stimulation of the immune system.

ZIKV-infected placental explants undergo apoptosis

To investigate whether ZIKV-induced replication, inflammation, and injury would result in cell death, we performed TUNEL assays 3 days after ZIKV infection to determine whether the explanted tissue underwent apoptosis (Fig. 5). DNase treatment was used as a positive control (Fig. 5a), while untreated, uninfected explants were used as negative control (Fig. 5b). ZIKV-BR-infected samples demonstrated prominent TUNEL staining, which appeared to be quantitatively comparable to the positive control sample (Fig. 5c). DENV infection resulted in lower TUNEL staining (Fig. 5d), which corroborates previous H&E data indicating that DENV2 causes less placental damage in this model.

Apoptosis was further confirmed by immunohistochemistry with cleaved caspase-3 antibodies. ZIKV-BR and DENV2 exhibited increased cleaved caspase 3 staining relative to the uninfected control, which is indicative of apoptotic cell death (Fig. 6a-f). Cleaved caspase 3 expression was higher in ZIKV-infected cultures than in DENV-infected cultures (Fig. 6h). Immunostaining was performed, and the stain was found to cover the

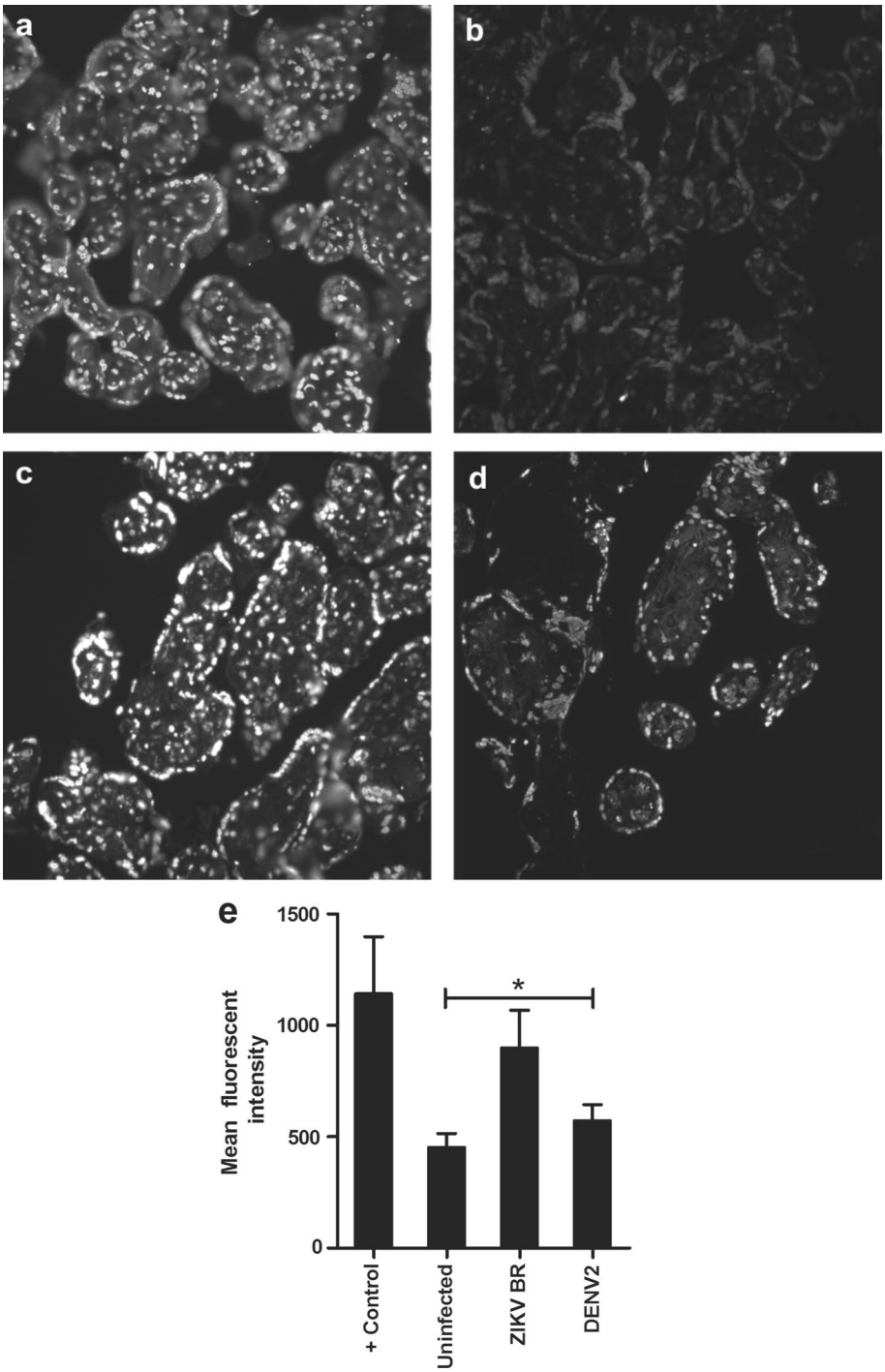

Fig. 5 Evaluation of ZIKV-induced apoptosis in placental explants measured by TUNEL assay. Infected explants on day 3 postinfection and uninfected explants were analyzed by TUNEL assay. Panel **a** represents the DNase-I-treated positive reaction control sample. Panel **b** represents the uninfected sample (control). TUNEL staining of placenta villi sections of ZIKV-BR (**c**) and DENV2-infected (**d**) tissue are shown. The images of TUNEL-positive cells were obtained at a magnification of 40x using an Olympus BX53 microscope system. Quantification was performed by measuring image intensity using Image-Pro® Plus software, version 7.0. One-way ANOVA and the Bonferroni correction were performed to determine statistical significance (*, $p < 0.05$; confidence interval, 95%)

chorionic villi. This result suggests that SCTs may be susceptible to apoptosis via active caspase-3 in ZIKV infections. SCTs cover chorionic villi and play a key role in the innate immune response and recruitment of NK cells [25]. Accordingly, previous studies that have investigated ZIKV tropism in several placental cell types have found ZIKV replication to be associated with abnormal tissue architecture, which could lead to the rupture of the placental barrier [16].

Cleaved-caspase-mediated apoptosis may result from an enhanced inflammatory response, such as the response involved in the TNF-α-TNFR signaling pathway. Because we detected increased expression of TNF-α in placental explants infected with ZIKV, we decided to investigate whether the observed apoptosis could be mediated by this cytokine. ZIKV-infected explants were treated with anti-TNF RII/TNFRSF1B neutralizing antibody, and cleaved caspase-3 activation was evaluated using IHC. Indeed,

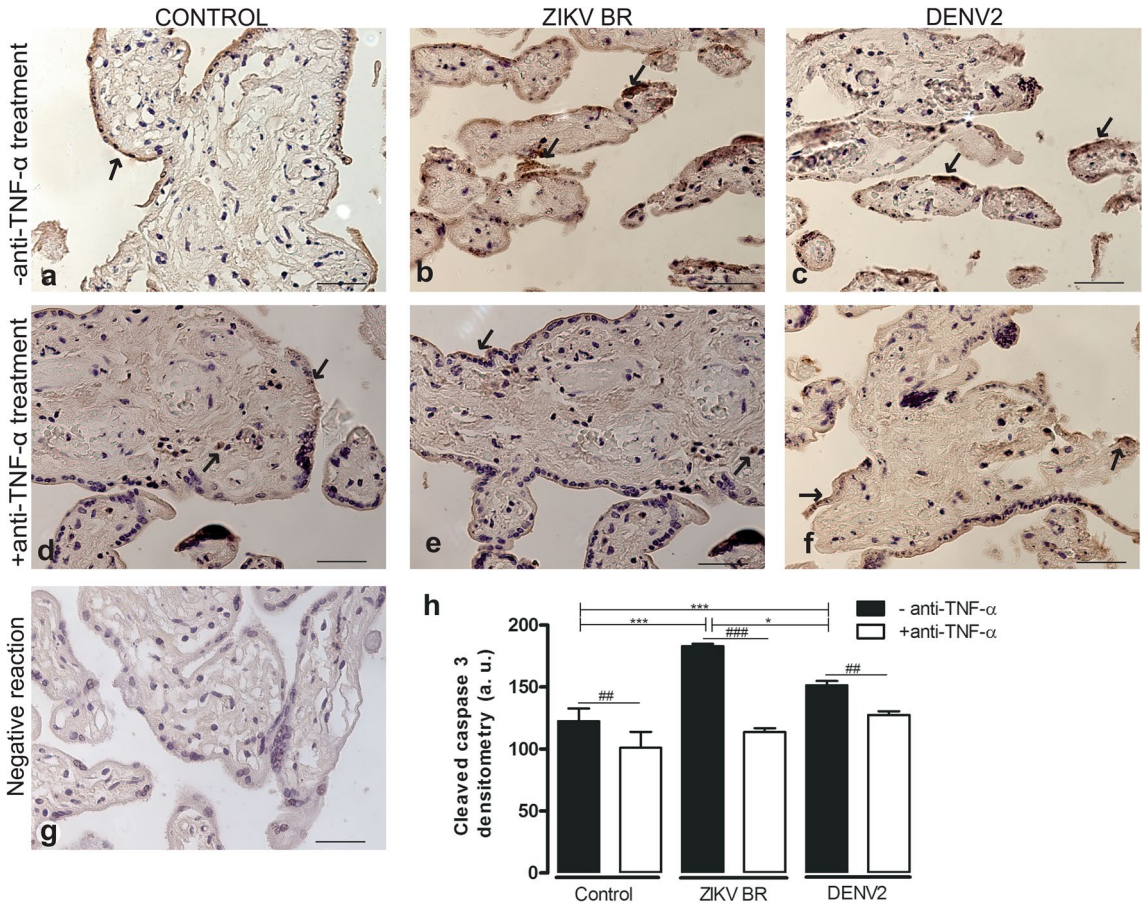

Fig. 6 ZIKV and DENV2 induce caspase-3 activation. Sections were stained with cleaved caspase-3 (**a-f**), as indicated by black arrows. Sections of uninfected samples (control) (**a**), ZIKV-infected tissues (**b**), and DENV2-infected tissues (**c**) are shown. Panels **d**-**f** show sections of uninfected samples (**d**) and ZIKV- or DENV2-infected explants treated with the anti-TNF-α antibody (panels **e** and **f** respectively). Panel **g** shows negative reaction controls in the absence of primary antibodies. Panel **k** shows the quantification densitometry analysis of cleaved caspase-3, which was performed using an Axioskop 2-Mot Plus Microscope (Carl Zeiss, Jena, Germany). AxioVision software was used for the qualitative analysis. One-Way ANOVA was performed to compare untreated groups (controls) to infected groups (*, $p < 0.01$; ***, $p < 0.001$). Two-way ANOVA was performed to compare treated groups to untreated groups with anti-TNF-α antibody ($^{###}$, $p < 0.001$). Scale bar: 10 μm

the anti-TNFR treatment significantly reduced cleaved caspase-3 staining, indicating that TNF-α-mediated apoptosis plays a significant role in tissue damage (Fig. 6d-f). TNFR neutralization also reduced cleaved caspase-3 staining in DENV-infected cultures, suggesting that both viruses are able to induce apoptosis, although lesion extension was found to be more severe when the tissues were infected with ZIKV. Some cell death was still observed after anti-TNFR treatment, suggesting that other mechanisms may also be involved in ZIKV-induced tissue damage. Previous studies have demonstrated that ZIKV infection in human neural progenitors (hNPCs) promotes increased caspase-3 expression, even in the presence of low levels of viral antigens [23]. These findings suggest that this pathway may be induced by ZIKV in different cell types and may be a relevant mechanism associated with congenital abnormalities.

We conclude that our placental tissue explant model is a valuable tool for the study of ZIKV interaction with the human placenta. We observed that placental explants are permissive to and support ZIKV and DENV2 infections for up to 120 hours. Because ZIKV is pathogenic to the human placenta, infected placental explants are amenable to different types of analysis and may therefore serve as a model in future research. Importantly, this model reinforces some critical observations made regarding ZIKV infection in other model systems and in patients [45, 49]. Due to its use of human placentas, this model provides crucial information to be applied to the clinical management of ZIKV infection, as well as to the development of preventive or therapeutic strategies against the deleterious effects of ZIKV on human embryos.

Acknowledgements The authors gratefully acknowledge the Brazilian National Institute of Science and Technology for Dengue Studies (INCT em Dengue), the São Paulo Research Foundation (FAPESP; Grant No. 2013/21719-3 to MLN) and the Brazilian National Research Council (CAPES) for their financial support.

Author contributions MRR and JBM performed the experiments, MRR, JBM, REM, PR, LBA, AN, SMO and MLN analyzed the data, MPP, LMM and LBA contributed reagents/materials/analysis tools, MRR, REM, LBA, SMO, AN and MLN wrote the paper, and PR, LBA, AHO, DMVO, SMO, AN and MLN planned the experiments.

References

1. Adams Waldorf KM, Stencel-Baerenwald JE, Kapur RP, Studholme C, Boldenow E, Vornhagen J, Baldessari A, Dighe MK, Thiel J, Merillat S, Armistead B, Tisoncik-Go J, Green RR, Davis MA, Dewey EC, Fairgrieve MR, Gatenby JC, Richards T, Garden GA, Diamond MS, Juul SE, Grant RF, Kuller L, Shaw DW, Ogle J, Gough GM, Lee W, English C, Hevner RF, Dobyns WB, Gale M, Rajagopal L (2016) Fetal brain lesions after subcutaneous inoculation of Zika virus in a pregnant nonhuman primate. Nat Med 22:1256–1259
2. Aliota MT, Caine EA, Walker EC, Larkin KE, Camacho E, Osorio JE (2016) Correction: Characterization of lethal Zika virus infection in AG129 mice. PLoS Negl Trop Dis 10:e0004750
3. Bayer A, Lennemann NJ, Ouyang Y, Bramley JC, Morosky S, Marques ET, Cherry S, Sadovsky Y, Coyne CB (2016) Type III interferons produced by human placental trophoblasts confer protection against Zika virus infection. Cell Host Microbe 19:705–712
4. Beckham JD, Pastula DM, Massey A, Tyler KL (2016) Zika virus as an emerging global pathogen: neurological complications of Zika virus. JAMA Neurol 73:875–879
5. Bowen JR, Quicke KM, Maddur MS, O'Neal JT, McDonald CE, Fedorova NB, Puri V, Shabman RS, Pulendran B, Suthar MS (2017) Zika virus antagonizes type I interferon responses during infection of human dendritic cells. PLoS Pathog 13:e1006164
6. Brey EM, Lalani Z, Johnston C, Wong M, McIntire LV, Duke PJ, Patrick CW (2003) Automated selection of DAB-labeled tissue for immunohistochemical quantification. J Histochem Cytochem 51:575–584
7. Calvet G, Aguiar RS, Melo AS, Sampaio SA, de Filippis I, Fabri A, Araujo ES, de Sequeira PC, de Mendonça MC, de Oliveira L, Tschoeke DA, Schrago CG, Thompson FL, Brasil P, Dos Santos FB, Nogueira RM, Tanuri A, de Filippis AM (2016) Detection and sequencing of Zika virus from amniotic fluid of fetuses with microcephaly in Brazil: a case study. Lancet Infect Dis 16:653–660
8. Carpentier PA, Dingman AL, Palmer TD (2011) Placental TNF-α signaling in illness-induced complications of pregnancy. Am J Pathol 178:2802–2810
9. Carteaux G, Maquart M, Bedet A, Contou D, Brugières P, Fourati S, Cleret de Langavant L, de Broucker T, Brun-Buisson C, Leparc-Goffart I, Mekontso Dessap A (2016) Zika virus associated with meningoencephalitis. N Engl J Med 374:1595–1596
10. Chaudhary V, Yuen KS, Chan JF, Chan CP, Wang PH, Cai JP, Zhang S, Liang M, Kok KH, Yuen KY, Jin DY (2017) Selective activation of type II interferon signaling by Zika virus NS5 protein. J Virol 91:e00163-17
11. Chutinimitkul S, Payungporn S, Theamboonlers A, Poovorawan Y (2005) Dengue typing assay based on real-time PCR using SYBR Green I. J Virol Methods 129:8–15
12. Corry J, Arora N, Good CA, Sadovsky Y, Coyne CB (2017) Organotypic models of type III interferon-mediated protection from Zika virus infections at the maternal–fetal interface. Proc Natl Acad Sci USA 114:9433–9438
13. Coyne CB, Lazear HM (2016) Zika virus—reigniting the TORCH. Nat Rev Microbiol 14:707–715
14. Cugola FR, Fernandes IR, Russo FB, Freitas BC, Dias JL, Guimarães KP, Benazzato C, Almeida N, Pignatari GC, Romero S, Polonio CM, Cunha I, Freitas CL, Brandão WN, Rossato C, Andrade DG, DeP Faria, Garcez AT, Buchpigel CA, Braconi CT, Mendes E, Sall AA, Zanotto PM, Peron JP, Muotri AR, Beltrão-Braga PC (2016) The Brazilian Zika virus strain causes birth defects in experimental models. Nature 534:267–271
15. Derricott H, Heazell AEP, Greenwood SL, Jones RL (2017) A novel in vitro model of villitis of unknown etiology demonstrates altered placental hormone and cytokine profile. Am J Reprod Immunol. https://doi.org/10.1111/aji.12725
16. El Costa H, Gouilly J, Mansuy JM, Chen Q, Levy C, Cartron G, Veas F, Al-Daccak R, Izopet J, Jabrane-Ferrat N (2016) ZIKA virus reveals broad tissue and cell tropism during the first trimester of pregnancy. Sci Rep 6:35296
17. Elovitz MA, Mrinalini C, Sammel MD (2006) Elucidating the early signal transduction pathways leading to fetal brain injury in preterm birth. Pediatr Res 59:50–55
18. Faria NR, Azevedo RDSD, Kraemer MUG, Souza R, Cunha MS, Hill SC, Thézé J, Bonsall MB, Bowden TA, Rissanen I, Rocco IM, Nogueira JS, Maeda AY, Vasami FGDS, Macedo FLL, Suzuki A, Rodrigues SG, Cruz ACR, Nunes BT, Medeiros DBA, Rodrigues DSG, Queiroz ALN, da Silva EVP, Henriques DF, da Rosa EST, de Oliveira CS, Martins LC, Vasconcelos HB, Casseb LMN, Simith DB, Messina JP, Abade L, Lourenço J, Alcantara LCJ, de Lima MM, Giovanetti M, Hay SI, de Oliveira RS, Lemos PDS, de Oliveira LF, de Lima CPS, da Silva SP, de Vasconcelos JM, Franco L, Cardoso JF, Vianez-Júnior JLDS, Mir D, Bello G, Delatorre E, Khan K, Creatore M, Coelho GE, de Oliveira WK, Tesh R, Pybus OG, Nunes MRT, Vasconcelos PFC (2016) Zika virus in the Americas: early epidemiological and genetic findings. Science 352:345–349
19. Fettke F, Schumacher A, Canellada A, Toledo N, Bekeredjian-Ding I, Bondt A, Wuhrer M, Costa SD, Zenclussen AC (2016) Maternal and fetal mechanisms of B cell regulation during pregnancy: human chorionic gonadotropin stimulates B cells to produce IL-10 while alpha-fetoprotein drives them into apoptosis. Front Immunol 7:495
20. Frank C, Cadar D, Schlaphof A, Neddersen N, Günther S, Schmidt-Chanasit J, Tappe D (2016) Sexual transmission of Zika virus in Germany, April 2016. Euro Surveill. https://doi.org/10.2807/1560-7917.ES.2016.21.23.30252
21. Fréour T, Mirallié S, Hubert B, Splingart C, Barrière P, Maquart M, Leparc-Goffart I (2016) Sexual transmission of Zika virus in an entirely asymptomatic couple returning from a Zika epidemic area, France, April 2016. Euro Surveill. https://doi.org/10.2807/1560-7917.ES.2016.21.23.30254
22. Garcia-Ruíz G, Flores-Espinosa P, Preciado-Martínez E, Bermejo-Martínez L, Espejel-Nuñez A, Estrada-Gutierrez G, Maida-Claros R, Flores-Pliego A, Zaga-Clavellina V (2015) In vitro progesterone modulation on bacterial endotoxin-induced production of IL-1β, TNFα, IL-6, IL-8, IL-10, MIP-1α, and MMP-9 in pre-labor human term placenta. Reprod Biol Endocrinol 13:115
23. Ghouzzi VE, Bianchi FT, Molineris I, Mounce BC, Berto GE, Rak M, Lebon S, Aubry L, Tocco C, Gai M, Chiotto AM, Sgrò F, Pallavicini G, Simon-Loriere E, Passemard S, Vignuzzi M, Gressens P, Di Cunto F (2016) ZIKA virus elicits P53 activation and

genotoxic stress in human neural progenitors similar to mutations involved in severe forms of genetic microcephaly and p53. Cell Death Dis 7:e2440
24. Girard S, Heazell AE, Derricott H, Allan SM, Sibley CP, Abrahams VM, Jones RL (2014) Circulating cytokines and alarmins associated with placental inflammation in high-risk pregnancies. Am J Reprod Immunol 72:422–434
25. Giugliano S, Petroff MG, Warren BD, Jasti S, Linscheid C, Ward A, Kramer A, Dobrinskikh E, Sheiko MA, Gale M, Golden-Mason L, Winn VD, Rosen HR (2015) Hepatitis C virus sensing by human trophoblasts induces innate immune responses and recruitment of maternal NK cells: potential implications for limiting vertical transmission. J Immunol 195:3737–3747
26. Gomes CP, Torloni MR, Gueuvoghlanian-Silva BY, Alexandre SM, Mattar R, Daher S (2013) Cytokine levels in gestational diabetes mellitus: a systematic review of the literature. Am J Reprod Immunol 69:545–557
27. Hamel R, Dejarnac O, Wichit S, Ekchariyawat P, Neyret A, Luplertlop N, Perera-Lecoin M, Surasombatpattana P, Talignani L, Thomas F, Cao-Lormeau VM, Choumet V, Briant L, Desprès P, Amara A, Yssel H, Missé D (2015) Biology of Zika virus infection in human skin cells. J Virol 89:8880–8896
28. Hamilton ST, Scott G, Naing Z, Iwasenko J, Hall B, Graf N, Arbuckle S, Craig ME, Rawlinson WD (2012) Human cytomegalovirus-induces cytokine changes in the placenta with implications for adverse pregnancy outcomes. PLoS One 7:e52899
29. Hamming OJ, Terczyńska-Dyla E, Vieyres G, Dijkman R, Jørgensen SE, Akhtar H, Siupka P, Pietschmann T, Thiel V, Hartmann R (2013) Interferon lambda 4 signals via the IFNλ receptor to regulate antiviral activity against HCV and coronaviruses. EMBO J 32:3055–3065
30. Heazell AE, Buttle HR, Baker PN, Crocker IP (2008) Altered expression of regulators of caspase activity within trophoblast of normal pregnancies and pregnancies complicated by preeclampsia. Reprod Sci 15:1034–1043
31. Helige C, Ahammer H, Hammer A, Huppertz B, Frank HG, Dohr G (2008) Trophoblastic invasion in vitro and in vivo: similarities and differences. Hum Reprod 23:2282–2291
32. Itinteang T, Tan ST, Guthrie S, Tan CE, McIntyre BC, Brasch HD, Day DJ (2011) A placental chorionic villous mesenchymal core cellular origin for infantile haemangioma. J Clin Pathol 64:870–874
33. Kotenko SV, Gallagher G, Baurin VV, Lewis-Antes A, Shen M, Shah NK, Langer JA, Sheikh F, Dickensheets H, Donnelly RP (2003) IFN-lambdas mediate antiviral protection through a distinct class II cytokine receptor complex. Nat Immunol 4:69–77
34. Kurman RJ, Young RH, Norris HJ, Main CS, Lawrence WD, Scully RE (1984) Immunocytochemical localization of placental lactogen and chorionic gonadotropin in the normal placenta and trophoblastic tumors, with emphasis on intermediate trophoblast and the placental site trophoblastic tumor. Int J Gynecol Pathol 3:101–121
35. Lanciotti RS, Kosoy OL, Laven JJ, Velez JO, Lambert AJ, Johnson AJ, Stanfield SM, Duffy MR (2008) Genetic and serologic properties of Zika virus associated with an epidemic, Yap state, micronesia, 2007. Emerg Infect Dis 14:1232–1239
36. Lash GE, Otun HA, Innes BA, Kirkley M, De Oliveira L, Searle RF, Robson SC, Bulmer JN (2006) Interferon-gamma inhibits extravillous trophoblast cell invasion by a mechanism that involves both changes in apoptosis and protease levels. FASEB J 20:2512–2518
37. Lazear HM, Govero J, Smith AM, Platt DJ, Fernandez E, Miner JJ, Diamond MS (2016) A mouse model of Zika virus pathogenesis. Cell Host Microbe 19:720–730
38. Lee HC, Narayanan S, Park SJ, Seong SY, Hahn YS (2014) Transcriptional regulation of IFN-λ genes in hepatitis C virus-infected hepatocytes via IRF-3·IRF-7·NF-κB complex. J Biol Chem 289:5310–5319
39. Leisser C, Saleh L, Haider S, Husslein H, Sonderegger S, Knöfler M (2006) Tumour necrosis factor-alpha impairs chorionic gonadotrophin beta-subunit expression and cell fusion of human villous cytotrophoblast. Mol Hum Reprod 12:601–609
40. Librach CL, Feigenbaum SL, Bass KE, Cui TY, Verastas N, Sadovsky Y, Quigley JP, French DL, Fisher SJ (1994) Interleukin-1 beta regulates human cytotrophoblast metalloproteinase activity and invasion in vitro. J Biol Chem 269:17125–17131
41. Malkki H (2016) CNS infections: mouse studies confirm the link between Zika virus infection and microcephaly. Nat Rev Neurol 12:369
42. McEwan M, Lins RJ, Munro SK, Vincent ZL, Ponnampalam AP, Mitchell MD (2009) Cytokine regulation during the formation of the fetal–maternal interface: focus on cell–cell adhesion and remodelling of the extra-cellular matrix. Cytokine Growth Factor Rev 20:241–249
43. Meager A, Visvalingam K, Dilger P, Bryan D, Wadhwa M (2005) Biological activity of interleukins-28 and -29: comparison with type I interferons. Cytokine 31:109–118
44. Melo AS, Aguiar RS, Amorim MM, Arruda MB, Melo FO, Ribeiro ST, Batista AG, Ferreira T, Dos Santos MP, Sampaio VV, Moura SR, Rabello LP, Gonzaga CE, Malinger G, Ximenes R, de Oliveira-Szejnfeld PS, Tovar-Moll F, Chimelli L, Silveira PP, Delvechio R, Higa L, Campanati L, Nogueira RM, Filippis AM, Szejnfeld J, Voloch CM, Ferreira OC, Brindeiro RM, Tanuri A (2016) Congenital Zika virus infection: beyond neonatal microcephaly. JAMA Neurol 73:1407–1416
45. Miner JJ, Cao B, Govero J, Smith AM, Fernandez E, Cabrera OH, Garber C, Noll M, Klein RS, Noguchi KK, Mysorekar IU, Diamond MS (2016) Zika virus infection during pregnancy in mice causes placental damage and fetal demise. Cell 165:1081–1091
46. Mlakar J, Korva M, Tul N, Popović M, Poljšak-Prijatelj M, Mraz J, Kolenc M, Resman Rus K, Vesnaver Vipotnik T, Fabjan Vodušek V, Vizjak A, Pižem J, Petrovec M, Avšič Županc T (2016) Zika virus associated with microcephaly. N Engl J Med 374:951–958
47. Moser G, Gauster M, Orendi K, Glasner A, Theuerkauf R, Huppertz B (2010) Endoglandular trophoblast, an alternative route of trophoblast invasion? Analysis with novel confrontation co-culture models. Hum Reprod 25:1127–1136
48. Musso D, Gubler DJ (2016) Zika Virus. Clin Microbiol Rev 29:487–524
49. Noronha L, Zanluca C, Azevedo ML, Luz KG, Santos CN (2016) Zika virus damages the human placental barrier and presents marked fetal neurotropism. Mem Inst Oswaldo Cruz 111:287–293
50. Onoguchi K, Yoneyama M, Takemura A, Akira S, Taniguchi T, Namiki H, Fujita T (2007) Viral infections activate types I and III interferon genes through a common mechanism. J Biol Chem 282:7576–7581
51. Otun HA, Lash GE, Innes BA, Bulmer JN, Naruse K, Hannon T, Searle RF, Robson SC (2011) Effect of tumour necrosis factor-α in combination with interferon-γ on first trimester extravillous trophoblast invasion. J Reprod Immunol 88:1–11
52. Pacanowski M, Amur S, Zineh I (2012) New genetic discoveries and treatment for hepatitis C. JAMA 307:1921–1922
53. Panchaud A, Stojanov M, Ammerdorffer A, Vouga M, Baud D (2016) Emerging role of Zika virus in adverse fetal and neonatal outcomes. Clin Microbiol Rev 29:659–694
54. Pantoja P, Pérez-Guzmán EX, Rodríguez IV, White LJ, González O, Serrano C, Giavedoni L, Hodara V, Cruz L, Arana T, Martínez MI, Hassert MA, Brien JD, Pinto AK, de Silva A, Sariol CA (2017) Zika virus pathogenesis in rhesus macaques is unaffected by pre-existing immunity to dengue virus. Nat Commun 8:15674
55. Pontillo A, Girardelli M, Agostinis C, Masat E, Bulla R, Crovella S (2013) Bacterial LPS differently modulates inflammasome gene

expression and IL-1β secretion in trophoblast cells, decidual stromal cells, and decidual endothelial cells. Reprod Sci 20:563–566
56. Quicke KM, Bowen JR, Johnson EL, McDonald CE, Ma H, O'Neal JT, Rajakumar A, Wrammert J, Rimawi BH, Pulendran B, Schinazi RF, Chakraborty R, Suthar MS (2016) Zika virus infects human placental macrophages. Cell Host Microbe 20:83–90
57. Rabaan AA, Bazzi AM, Al-Ahmed SH, Al-Ghaith MH, Al-Tawfiq JA (2017) Overview of Zika infection, epidemiology, transmission and control measures. J Infect Public Health 10:141–149
58. Raghupathy R, Kalinka J (2008) Cytokine imbalance in pregnancy complications and its modulation. Front Biosci 13:985–994
59. Rossi SL, Tesh RB, Azar SR, Muruato AE, Hanley KA, Auguste AJ, Langsjoen RM, Paessler S, Vasilakis N, Weaver SC (2016) Characterization of a novel murine model to study Zika virus. Am J Trop Med Hyg 94:1362–1369
60. Roth I, Corry DB, Locksley RM, Abrams JS, Litton MJ, Fisher SJ (1996) Human placental cytotrophoblasts produce the immunosuppressive cytokine interleukin 10. J Exp Med 184:539–548
61. Roth I, Fisher SJ (1999) IL-10 is an autocrine inhibitor of human placental cytotrophoblast MMP-9 production and invasion. Dev Biol 205:194–204
62. Siwetz M, Blaschitz A, El-Heliebi A, Hiden U, Desoye G, Huppertz B, Gauster M (2016) TNF-α alters the inflammatory secretion profile of human first trimester placenta. Lab Invest 96:428–438
63. Tabata T, Petitt M, Puerta-Guardo H, Michlmayr D, Wang C, Fang-Hoover J, Harris E, Pereira L (2016) Zika virus targets different primary human placental cells, suggesting two routes for vertical transmission. Cell Host Microbe 20:155–166
64. Turmel JM, Abgueguen P, Hubert B, Vandamme YM, Maquart M, Le Guillou-Guillemette H, Leparc-Goffart I (2016) Late sexual transmission of Zika virus related to persistence in the semen. Lancet 387:2501
65. Vargas-Rojas MI, Solleiro-Villavicencio H, Soto-Vega E (2016) Th1, Th2, Th17 and Treg levels in umbilical cord blood in preeclampsia. J Matern Fetal Neonatal Med 29:1642–1645
66. Vermillion MS, Lei J, Shabi Y, Baxter VK, Crilly NP, McLane M, Griffin DE, Pekosz A, Klein SL, Burd I (2017) Intrauterine Zika virus infection of pregnant immunocompetent mice models transplacental transmission and adverse perinatal outcomes. Nat Commun 8:14575
67. Vićovac L, Jones CJ, Aplin JD (1995) Trophoblast differentiation during formation of anchoring villi in a model of the early human placenta in vitro. Placenta 16:41–56
68. Vorou R (2016) Zika virus, vectors, reservoirs, amplifying hosts, and their potential to spread worldwide: what we know and what we should investigate urgently. Int J Infect Dis 48:85–90
69. Wikan N, Smith DR (2016) Zika virus: history of a newly emerging arbovirus. Lancet Infect Dis 16:e119–e126
70. Wilczyński JR, Tchórzewski H, Banasik M, Głowacka E, Wieczorek A, Lewkowicz P, Malinowski A, Szpakowski M, Wilczyński J (2003) Lymphocyte subset distribution and cytokine secretion in third trimester decidua in normal pregnancy and preeclampsia. Eur J Obstet Gynecol Reprod Biol 109:8–15
71. Winkler CW, Woods TA, Rosenke R, Scott DP, Best SM, Peterson KE (2017) Sexual and vertical transmission of Zika virus in anti-interferon receptor-treated Rag1-deficient mice. Sci Rep 7:7176
72. Wu KY, Zuo GL, Li XF, Ye Q, Deng YQ, Huang XY, Cao WC, Qin CF, Luo ZG (2016) Vertical transmission of Zika virus targeting the radial glial cells affects cortex development of offspring mice. Cell Res 26:645–654